# Process Design of Laser Forming for Three-Dimensional Thin Plates

**Jin Cheng***

**Y. Lawrence Yao**

Department of Mechanical Engineering,
Columbia University,
New York, NY 10027

*Extensive efforts have been made in analyzing and predicting laser forming processes of sheet metal. Process design, on the other hand, is concerned with determination of laser scanning paths and laser heat condition given a desired shape. This paper presents an approach for process design of laser forming of thin plates with doubly curved shapes. The important feature of this method is that it first calculates the strain field required to form the shape. Scanning paths are decided based on the concept of in-plane strain, bending strain, principal minimal strain and temperature gradient mechanism of laser forming. Heating condition is determined by a lumped method. Effectiveness of the approach is numerically and experimentally validated through two different doubly curved shapes.* [DOI: 10.1115/1.1751187]

## 1 Introduction

Extensive research has been done to analyze deformation and residual stress given material properties, laser scanning paths, and heating condition. Numerical and experimental investigations have been carried out to better understand process mechanisms and the effects of key process parameters on dimension and mechanical properties of the formed parts [1–3]. Temperature and strain-rate dependent material properties were compiled and considered in the numerical models developed for concave, convex, and tube laser-forming processes, and nonlinear relationships including appropriate flow rule and yield criterion were specified for plastic deformation [4–6]. For laser forming to become a more practical process, the issue of process synthesis needs to be addressed. To date, however, few studies in process design of laser forming have been reported. The process design can be divided into two steps. The first step is to decide where and how to apply laser energy and the second step is to decide how much energy to impart.

Line heating, based on which laser forming was inspired, has been used to form ship hulls and correct unwanted distortions due to welding and other heat processes. It is heavily dependent on experience of skilled workers, and therefore research has been carried out for the process design of line heating. Ueda et al. [7–9] determined the heating paths by developing a desired shape onto a flat one, computing the magnitudes of inherent strains, selecting heating regions based on the distribution of inherent strains, and concentrating the strains to the selected regions. It is not entirely clear what central role the introduction of the inherent strains plays. It is also not shown that the large deformation elastic FEM used for the planar development is valid for an electroplastic problem like line heating. Jang, et al. [10] developed an algorithm to determine the heating lines based on the principal curvatures of the deflection difference surface that represents the shape difference between a desirable shape and an intermittent shape fabricated from the original planar shape. Candidate heating regions are selected by grouping the points where principal curvature is larger. Which side of sheet metal to heat is also determined based on classification of surfaces according to Gaussian and mean curvatures. The method, however, employed many empirical factors and the way they classified the surface limited the applications for complex three-dimensional plate forming.

More recently, efforts have been made in process design of laser forming. Shimizu [11] applied generic algorithms (GAs) to a dome shaped sheet to determine a heat condition assuming the laser scanning paths are known. He used discrete values to represent the heat condition and the result is less flexible and natural. It also experienced difficulty when an experimental validation of the result was attempted. Yu et al., [12] presented algorithms for optimal development (flattening) of doubly curved surfaces into a planar shape in the sense that the strain from the surface to its planar development is minimized. The development process was modeled by in-plane strain (stretching) from the curved surface to its planar development. The distribution of the appropriate minimum strain field was obtained by solving a constrained nonlinear programming problem. No scanning paths were determined nor direct connections with laser forming were made.

Recognizing the complexities involved in process design of laser forming, Cheng and Yao [13] developed a synthesis process for laser forming of a class of 2D shaped sheet metal. The synthesis process is based on GAs. Number of laser scans, distance between adjacent scans, laser scanning speed and power were treated as decision variables during design cycles. The approach used several analytical equations based on experiment and numerical modeling to predict the geometry change occurring in straight-line laser forming. Given a desired 2D shape, the approach was shown to be effective in determining optimal values of these decision variables to minimize the difference between the desired and laser formed shape. Similarly, Liu and Yao [14] developed an optimal and robust approach for process design of the same class of 2D laser forming. Response surface methodology was used as an optimization tool and integer design variables were properly dealt with. The propagation of error technique was built into the design process as an additional response to be optimized via desirability function and hence make the design robust. This design scheme was validated in several cases numerically and experimentally. Both methods, however, are limited to the process design of the class of 2D shapes.

This paper presents a methodology to design laser scanning paths and heating condition of laser forming for a general class of three-dimensional shapes—thin plates whose mid-plane is represented by doubly curved surfaces. An overall strategy is laid out first, followed by detailed description of each steps of the methodology. Two typical shapes for ship hulls or aerospace structures,

*Currently with School of Mechanical and Materials Engineering, Washington State University.

Contributed by the Manufacturing Engineering Division for publication in the JOURNAL OF MANUFACTURING SCIENCE AND ENGINEERING. Manuscript received December 2002; Revised October 2003. Associate Editor: A. Shih.

pillow and saddle shapes are focused on. The methodology is aided by finite element method (FEM) and validated by forming experiments.

## 2 Overall Strategy

For most manufacturing processes, process design amounts to determination of process parameters such as force, speed, depth of cut, and rolling reduction. It is typically not difficult to determine tool path either because presence of hard tooling makes it obvious such as in machining, rolling, and stamping, or because nature of a process makes it obvious such as in laser machining and laser welding. For example, in machining of free-form surfaces, cutter paths are readily determined which are closely related with the desired shape. In forming rolling, the trajectory of forming rolls closely resembles the shape to be formed. In stamping, die shape closely resembles the part to be stamped except a certain consideration for spring-back.

The process design of laser forming, however, differs from these processes in that the laser scanning path is not necessarily directly related with the desired shape, especially for 3D shapes. Generally speaking, the regions of a shape, which require larger deformation, need to be scanned and scanned more but exact scanning paths, i.e., orientations, linear or curved, are not obvious. This is because laser forming is a non-contact forming process without external forces or hard tooling, and the relation between heating and deformation is complex. In addition, the process design of laser forming, like all inverse problems, generally has multiple solutions for a given shape.

An overall strategy for process design of laser forming is presented which involves three steps. The first step is to determine a strain field that is required to obtain a desired shape from a planar shape or vise verse, the second step is to decide on laser scanning paths, and the third step is to decide on the heating condition (i.e., laser power levels and scanning velocities) for the determined strain field and scanning paths. Laser beam spot size is considered constant in this paper. Figure 1 summarizes the algorithms for these three steps. Doubly-curved thin plate shapes are considered which generally require both in-plane and bending strains to form.

Given a desired shape, large-deformation elastic FEM is applied to solve the planar development problem and obtain a strain field under displacement constraints. The displacement constraints are applied by compressing the doubly-curved thin plate between two analytical rigid plates, defining the displacement on one of the two analytical rigid plates and fixing the other. There is no friction between two analytical rigid plates and doubly-curved thin plate. The compression stops until the gap between the two analytical rigid plates is equal to the thickness of the doubly-curved thin plate. Therefore, displacement constraints are applied on all of the nodes on the doubly-curved thin plate. The reason using FEM instead of a geometric method is that surface development methods such as Yu et al., [12] based on differential geometry typically yield in-plane strain only while FEM calculates total strain which is then decomposed into in-plane and bending strains. The reason to use large-deformation FEM is that most of the deformations in development of three-dimensional shaped thin plate are greater than 5%. Therefore, appropriate stress and strain tensors have to be used. Elastic FEM is applied instead of elasto-plastic FEM because less material properties need to be specified. In fact, it will be shown that the planar development process is even independent of Young's modulus.

It is, however, impossible to duplicate exactly the strain field by laser forming. Therefore, the strain field is decomposed into in-plane and bending strains because it is well known that laser forming generates both. The direction and magnitude of minimal (compressive) principal in-plane and bending strains are further calculated since it is well known that the direction is perpendicular to laser scanning paths. It is this fact that is used to determine the scanning paths. If the principal minimal in-plane strain is significantly larger than principal minimal bending strain, scanning paths are chosen to be normal to principal in-plane strain direction and vice versa.

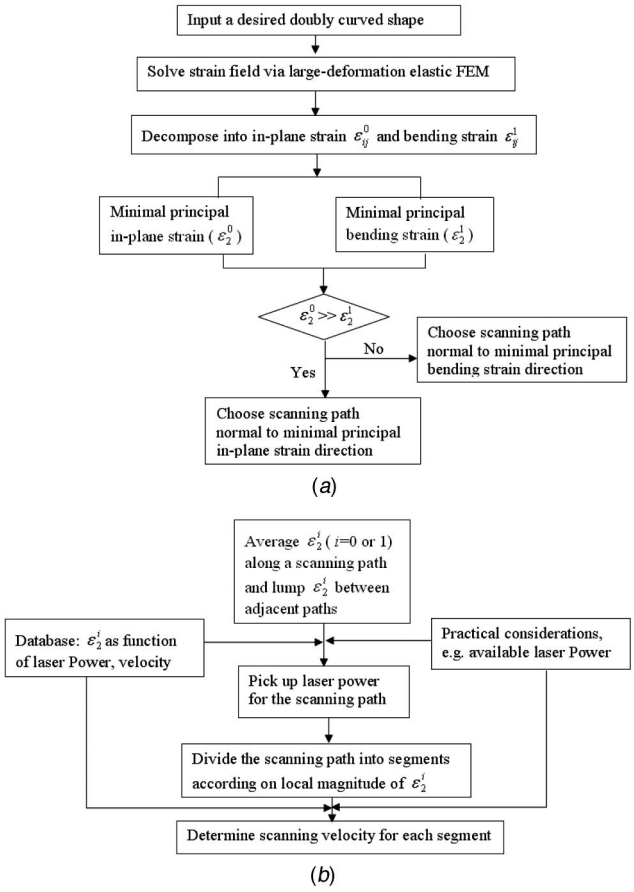


**Fig. 1 Overall strategy for determining (*a*) scanning paths and (*b*) heating condition**

Finally, the heating condition is determined. The required minimal principal strain between adjacent scanning paths is first lumped together. A database concerning the relationship between principal strains and laser power levels and scanning velocities is then consulted. A power level is chosen from the relationship together with practical considerations and corresponding scanning velocity is determined as a result.

In engineering applications, there exist two kinds of surfaces, developable surfaces and non-developable surfaces, which are also called singly and doubly curved surfaces, respectively. A singly curved surface has zero Gaussian curvature at all points and can be formed only by bending strain, while a doubly curved surface has non-zero Gaussian curvature at least in some region and generally requires both in-plane and bending strains to form. Surfaces of many engineering structures are commonly fabricated as doubly curved shapes to fulfill functional requirements such as hydrodynamic, aesthetic, or structural. For example, a large portion of the shell plates of ship hulls or airplane fuselages are doubly curved surfaces.

This paper illustrates the proposed strategy by applying it to two distinctive 3D shapes, a pillow and a saddle shape. Since this paper is concerned with thin plates, that is, $w(x,y,z,t) = w_o(x,y,t)$, where $w$ is deflection in the $z$ direction, the midplane of these two shapes is specified in terms of a cubic-spline sweep surface, respectively, and then extruded by a half of the plate thickness in both thickness directions. The sweep surfaces are generated by sweeping a cross-section curve $C(y)$, a cubic-spline curve, along an axis curve $A(x)$, another cubic-spline

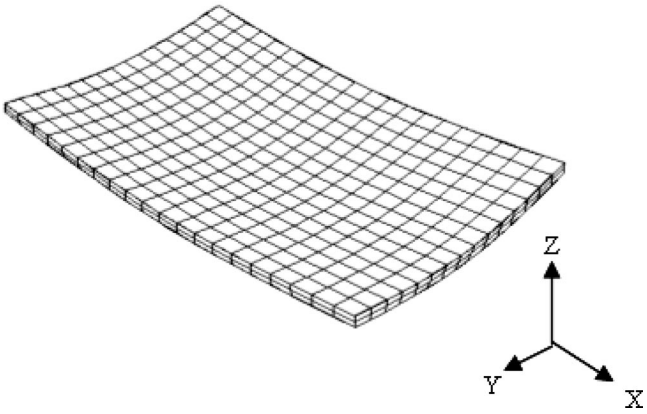


**Fig. 2 Desired shape I: pillow (dimension: 140*80*0.89 mm$^3$, magnification ×5 in thickness for viewing clarity)**

curve. The plane of the cross-section curve is kept on the $y$-$z$ plane. Then the sweep surface is defined by: $S(x,y)=A(x)+C(y)$ $x\in[0,140]$, $y\in[0,80]$ in mm. For both cases, $C(y)$ is defined as a piecewise cubic function with interior knots: (0, 0, 0), (0, 40, 5), and (0, 80, 0). This cubic function: $C_i(y)=a_iy^3+b_iy^2+c_iy+d_i$; $(i=1,2,3)$ has the following properties: $C(y)$ is piece wise cubic on [0, 80], and $C(y)$, $C'(y)$ and $C''(y)$ are continuous on [0, 80]. Similarly, $A(x)$ is defined by a piecewise cubic spline function with interior knots: (0, 0, 0), (70, 0, 5), and (140, 0, 0) for pillow shape, and (0, 0, 5), (70, 0, 0), and (140, 0, 5) for saddle shape. $A(x)$ has the same continuity properties as $C(y)$. The two desired shapes are shown in Figs. 2 and 3.

## 3 Strain Field Determination

As indicated in the overall strategy, the first step is to determine a strain field required to develop a desired shape to a planar shape, which is the opposite of developing a planar shape to the desired shape and therefore the found strain field has an opposite sign. A strain field required for such a planar development is solved by FEM. The type of FEM used is large-deformation elastic FEM.

The reason of opting for FEM instead of a geometrical method based on differential geometry is that the former gives a complete strain field throughout the plate, while the latter typically gives in-plane strain for a surface only. The reason of using large-deformation FEM is as follows. When the deflection (the normal component of the displacement vector), $w_0$, of the midplane is small compared with the plate thickness, $h$ ($w_0\leqslant 0.2h$), the Kirchhoff's linear plate bending theory gives sufficiently accurate results. The in-plane strain and the corresponding in-plane stress

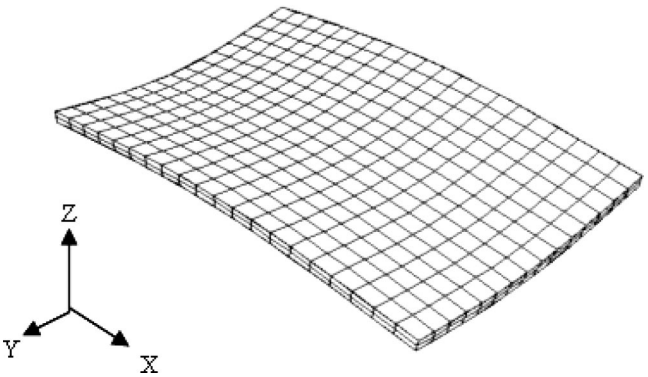


**Fig. 3 Desired shape II: saddle (dimension: 140*80*0.89 mm$^3$, magnification ×5 in thickness for viewing clarity)**

are neglected. However, if the magnitude of deflection increases beyond a certain level ($w_0\geqslant 0.3h$), these deflections are accompanied by stretching of the mid-plane. As the ratio $w_0/h$ further increases, the role of in-plane strain becomes more pronounced. In our case, $w_0/h$ reaches 5.6, therefore the nonlinear effects have to be taken into account. The reason why elastic FEM is applied instead of elasto-plastic FEM is that, the strain field development from the desired shape to a planar shape is purely geometrical, and should be independent of material properties including both elastic and plastic properties. Using elastic FEM requires only elastic properties such as Young's modules $E$ to be specified. Furthermore it is shown below that the strain field determination is independent of the value of $E$.

For thin plate deformation, deflection $w(x,y)$ is assumed to be equal to the deflection of the midplane, $w_0(x,y)$. The total strains of deflection can be expressed as follows.

$$\varepsilon_{xx}=\varepsilon^0_{xx}+\varepsilon^1_{xx}=\left[\frac{\partial u_0}{\partial x}+\frac{1}{2}\left(\frac{\partial w_0}{\partial x}\right)^2\right]+\left[-z\frac{\partial^2 w_0}{\partial x^2}\right]$$

$$\varepsilon_{yy}=\varepsilon^0_{yy}+\varepsilon^1_{yy}=\left[\frac{\partial v_0}{\partial y}+\frac{1}{2}\left(\frac{\partial w_0}{\partial y}\right)^2\right]+\left[-z\frac{\partial^2 w_0}{\partial y^2}\right]$$

$$\gamma_{xy}=\gamma^0_{xy}+\gamma^1_{xy}=\left[\frac{\partial u_0}{\partial y}+\frac{\partial v_0}{\partial x}+\frac{\partial w_0}{\partial x}\frac{\partial w_0}{\partial y}\right]+\left[-2z\frac{\partial^2 w_0}{\partial x\partial y}\right] \quad (1)$$

where $u_0$, $v_0$, and $w_0$ are the displacement at midplane, $\varepsilon_{xx}$, $\varepsilon_{yy}$, and $\gamma_{xy}$ are total strains, and $\varepsilon^0_{xx}$, $\varepsilon^0_{yy}$, and $\gamma^0_{xy}$ are in-plane strains, and $\varepsilon^1_{xx}$, $\varepsilon^1_{yy}$, and $\gamma^1_{xy}$ are bending strains.

For small deflection of thin plates, it is assumed that $u_0$ and $v_0$ are zero and slopes $\partial w_0/\partial x$ and $\partial w_0/\partial y$ are small. Therefore, the in-plane strains $\varepsilon^0_{xx}$, $\varepsilon^0_{yy}$, and $\gamma^0_{xy}$ are zero and the total strains only contain the bending strains. As seen, the bending strains equal to product of position in the thickness direction $z$ and a term which approximately equals to the curvature at that point, that is,

$$\varepsilon_{xx}=\varepsilon^1_{xx}=-z\frac{\partial^2 w_0}{\partial x^2}=zR_x, \quad \varepsilon_{yy}=\varepsilon^1_{yy}=-z\frac{\partial^2 w_0}{\partial y^2}=zR_y,$$

$$\gamma_{xy}=\gamma^1_{xy}=-2z\frac{\partial^2 w_0}{\partial x\partial y}=-2zR_{xy} \quad (2)$$

where, $R_x$ and $R_y$ are approximately the curvature along the $x$-axis and $y$-axis, respectively. $R_{xy}$ can be defined as a twisting curvature, which represents the warping of the $x$-$y$ plane. Given a desired shape, $R_x$, $R_y$ and $R_{xy}$ are known and therefore the total strains only depend on $z$, independent of any material properties, In particular, they can be determined independent of Young's modulus in the large-deformation elastic FEM.

For large deflection of thin plates, the bending strains are the same as in Eq. (2) and the in-plane strains, $\varepsilon^0_{xx}$, $\varepsilon^0_{yy}$, and $\gamma^0_{xy}$ can be expressed by Hooke's law as

$$\varepsilon^0_{xx}=\frac{1}{h}\left(\frac{\partial^2\varphi}{\partial y^2}-\nu\frac{\partial^2\varphi}{\partial x^2}\right), \quad \varepsilon^0_{yy}=\frac{1}{h}\left(\frac{\partial^2\varphi}{\partial x^2}-\nu\frac{\partial^2\varphi}{\partial y^2}\right),$$

$$\text{and} \quad \gamma^0_{xy}=-\frac{2(1+\nu)}{h}\frac{\partial^2\varphi}{\partial x\partial y} \quad (3)$$

where $\varphi$ is stress function $\phi$ divided by Young's modules $E$, $h$ is plate thickness, and $\nu$ is Poisson ratio. $\varphi$ can be calculated by solving the following governing equations for thin plate deflection under appropriate boundary conditions.

$$\frac{\partial^4\varphi}{\partial x^4}+2\frac{\partial^4\varphi}{\partial x^2\partial y^2}+\frac{\partial^4\varphi}{\partial y^4}=h\left[\left(\frac{\partial^2 w_0}{\partial x\partial y}\right)^2-\frac{\partial^2 w_0}{\partial x^2}\frac{\partial^2 w_0}{\partial y^2}\right]$$

$$\frac{\partial^4 w_0}{\partial x^4}+2\frac{\partial^4 w_0}{\partial x^2\partial y^2}+\frac{\partial^4 w_0}{\partial y^4}=\frac{1}{D'}\left[P'+\frac{\partial^2\varphi}{\partial y^2}\frac{\partial^2 w_0}{\partial x^2}+\frac{\partial^2\varphi}{\partial x^2}\frac{\partial^2 w_0}{\partial y^2}-2\frac{\partial^2\varphi}{\partial x\partial y}\frac{\partial^2 w_0}{\partial x\partial y}\right] \quad (4)$$

where $D'=h^3/12(1-\nu^2)$ is flexural rigidity $D$ divided by $E$, and $P'(x,y)$ is lateral load in $z$ direction $P(x,y)$ divided by $E$. More detailed derivation of the equations is listed in the Appendix. As seen from Eqs. (3) and (4), once a desired shape is given, that is, deflection $w_0$, and curvatures $\partial^2 w_0/\partial x^2$, $\partial^2 w_0/\partial y^2$, and $\partial^2 w_0/\partial x\partial y$ are known, $\varphi$ and $P'$ and in turn the in-plane strains $\varepsilon^0_{xx}$, $\varepsilon^0_{yy}$, and $\gamma^0_{xy}$ can be calculated under appropriate boundary conditions and the calculation is independent of Young's modulus. As seen in Eq. (3), they do depend on Poisson ratio, which is geometrical property. In summary, it is shown that, given a desired shape of thin plate, a strain field required to develop the shape to a planar shape can be determined independent of any material properties including Young's modules, no matter small or large deformation is concerned. In other words, the proposed elastic FEM is valid to obtain a strain field for an elastic-plastic problem like laser forming. The large-deformation elastic FEM is carried out using commercial code ABAQUS. It is verified that different values of Young's modules yielded the same strain field given everything else the same.

Laser forming, however, is unable to exactly duplicate the strain field since laser forming only effects a certain strain distribution. But it is known that the doubly curved shapes under consideration can be developed by in-plane and bending strains and laser forming generally yields in-plane and bending strains. As a result, the total strains $\varepsilon_{ij}$ obtained via FEM are decomposed into in-plane strain $\varepsilon^1_{ij}$, and bending strain, $\varepsilon^0_{ij}$, as follows.

$$\varepsilon^0_{ij}=\frac{1}{h}\int_{h/2}^{-h/2}\varepsilon_{ij}dz$$

$$\varepsilon^1_{ij}=\frac{2}{h^2}\int_{h/2}^{-h/2}z(\varepsilon_{ij}-\varepsilon^0_{ij})dz \quad (5)$$

As seen, the in-plane strain arises from the integration of the total strain along thickness $h$. For thin plates, however, the in-plane strain equals to the midplane strain because the bending strain varies linearly with $z$ as seen from Eq. (1) and $w(x,y,z)=w_o(x,y)$.

After a strain field is determined and decomposed into in-plane and bending strain components, the next step in the overall strategy is to find the direction and magnitude of minimal principal (compressive) strain for both, in order to determine laser scanning paths (Fig. 1). It is well known that under the temperature gradient mechanism, highest compressive strains occur in the direction perpendicular to a laser scanning path. Therefore laser scanning paths will be placed perpendicular to the direction of minimal principal strain. The principal strain and principal direction are readily determined by the well-known plane-strain formulation. Figure 4 shows magnitude contour plots of minimal principal in-plane and bending strain for the pillow shape and Fig. 5 for the saddle shape, respectively.

## 4 Scanning Path Determination

As discussed early, the type of given doubly curved shapes requires both in-plane and bending strains to general and laser forming generally results both in-plane and bending strains. Furthermore, the highest compressive strains occur in a direction perpendicular to a scanning path. Therefore a scanning path should be perpendicular to the direction of the in-plane strain if its magnitude is much greater than that of the bending strain (Fig. 1) as in the case of many thin plates. Examining Figs. 4 and 5 confirms that. As seen, for both shapes, the magnitude of the in-plane strain is an order of magnitude higher than the bending strain. This is

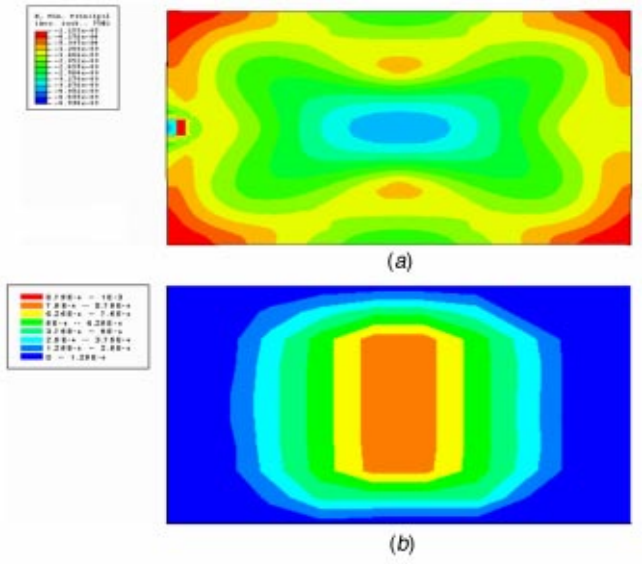


**Fig. 4 (*a*) Minimal principal in-plane strain, and (*b*) minimal principal bending strain for the pillow shape (dimension: 140*80*0.89 mm$^3$)**

expected for the thin plates under consideration. Figure 6 shows vector plots of minimal principal in-plane strains for the pillow and saddle shapes, where the orientation of the vectors represents the direction and the length of the vectors the magnitude of the minimal principal in-plane strain. Scanning paths will be traced perpendicular to the vectors representing the minimal principal in-plane strain. Figure 7 shows a set of scanning paths, superposed on the vector field of minimal principal in-plane strain of pillow and saddle shapes, respectively.

In determining the spacing of scanning paths, a number of considerations are given. In general, the smaller the spacing, more precise the desired shapes can be formed and lower energy input is required for each path. On the other hand, it will take longer to form the shapes and adjacent paths can no longer be assumed

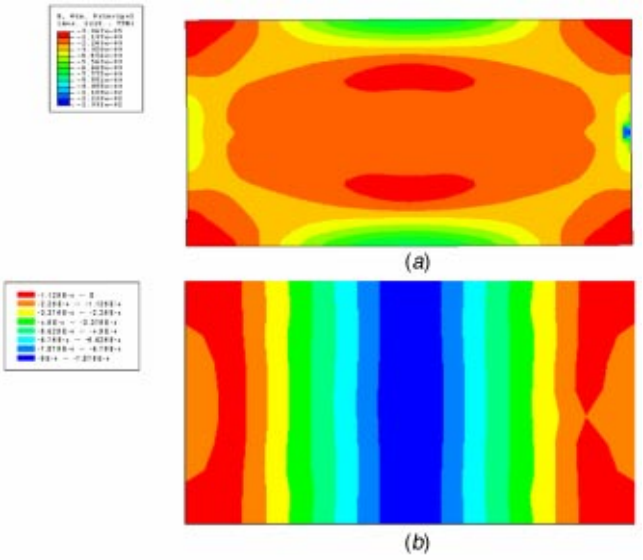


**Fig. 5 (*a*) Minimal principal in-plane strain, and (*b*) minimal principal bending strain for the saddle shape (dimension: 140*80*0.89 mm$^3$)**

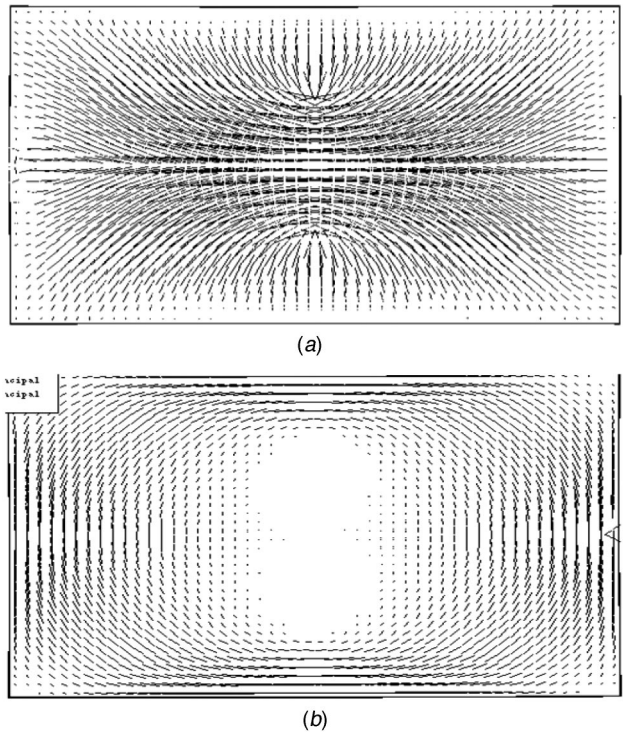

**Fig. 6 Vector plots of minimal principal in-plane strain for (*a*) pillow shape, and (*b*) saddle shape (the orientation of segments indicates strain direction and length of segments indicates strain magnitude)**

independent with each other. The independence is paid attention to because when a heat condition is determined as seen in the next section, it is based on a database which is constructed using independent scans. In addition, non-uniform spacing is normally desirable because strains vary from one region to the other. The larger strains are, the smaller the spacing should be. Roughly speaking, spacing between two adjacent paths, $d_{paths}$, should be equal to strain generated by laser forming, $\varepsilon_{laser}$, multiplied by laser beam spot size, $d_{laser}$ (because a vast majority of the laser-generated stain is within the region covered by the laser spot), divided by the average principal minimal strain $\varepsilon_2^i$ over the spacing, that is:

$$d_{paths}=\frac{\varepsilon_{laser}d_{laser}}{ave(\varepsilon_2^i)} \tag{6}$$

Another practical consideration is where to initial and terminate a scanning path. For this work, a threshold is applied so that only 90% of the total area will be scanned. The 10% excluded represents the regions having smallest strains. For the pillow shape, the 10% concentrates at the corners while for the saddle shape at the center (Fig. 7). Note that the edges of the planar developments of both shapes shown in Figs. 6 and 7 are somewhat curved, which suggests how the planar plates should be cut before laser scanning. It is expected that if the desired shapes deflect more, more curved edges will be observed.

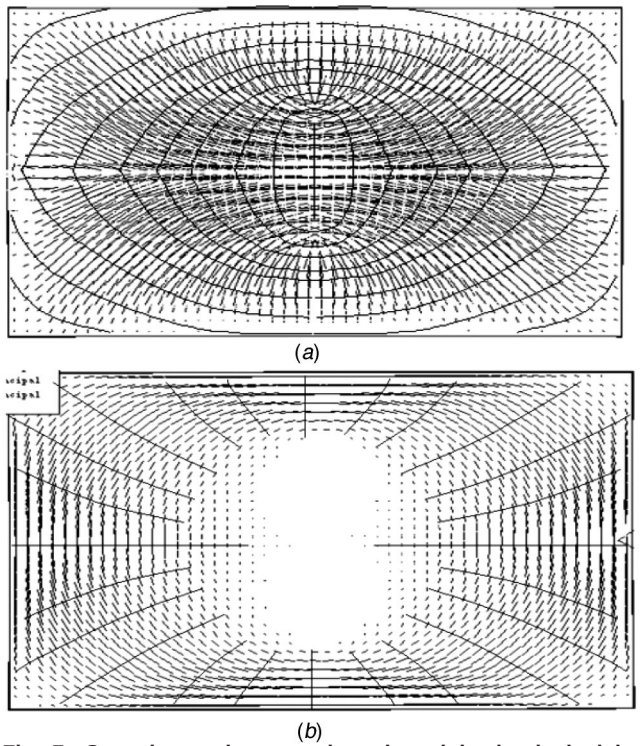

**Fig. 7 Scanning paths normal to the minimal principal in-plane strain for (*a*) pillow shape, and (*b*) saddle shape**

## 5 Heating Condition Determination

After determination of the scanning paths, the next step is to determine a heating condition, that is, a required energy input, which depends on laser power and laser scanning velocity if laser beam spot size and work material are given. Obviously there are multiple solutions to this problem because many power and velocity combinations may meet the requirement. The strategy proposed in this work is outlined in Fig. 1(*b*) and summarized below.

The in-plane or bending minimal principal strains are first averaged along a scanning path and lumped between adjacent paths for all the paths determined above. Laser forming conditions are chosen such that the in-plane and bending strains after laser forming are equal to these in-plane and bending strains. In this study, the averaged in-plane and bending strains are then entered into a database which contains relationships between minimal principal in-plane and bending strains averaged within the heating zone (i.e., the laser beam spot size) vs. laser power and scanning velocity as shown in Fig. 8. The database is established using FEM of independent scans and detail of the modeling is seen in [13]. A series of laser forming analyses were conduct to get relationship between in-plane strain and bending strain and laser heating conditions. The total strains from FEM are decomposed into in-plane and bending strain by Eq. (5). The material is 1010 steel and sheet thickness is 0.89 mm the same as the desired shapes. Given the averaged strain, a horizontal intersection of the surfaces shown in Fig. 8 can be made, which represents a set of laser power and scanning velocity combinations. Choose a laser power level from the intersection for the scan such that laser power levels chosen for all scans are feasible to be realized by existing laser forming equipment. There is a single power level for each path. Lastly, each path is divided into a few segments and scanning velocity of each segment is determined based on the local strain and laser power chosen for the path, again using Fig. 8. The heating condition for the two desired shapes is decided following the procedure outlined above. The results are shown in Fig. 9, where the determined scanning velocity and laser power levels are indicated along the scanning paths superposed on magnitude contour plots. Due to symmetry, only a quarter of the desired shapes are shown.

Experiments are conducted based on the scanning paths and heating condition determined above on 1010 steel sheets of size 140 by 80 by 0.89 mm. The laser system used is a PRC-1500 $CO_2$ laser, which has a maximum output power of 1500 W. Motion of workpiece is controlled by Unidex MMI500 motion control system, which allows easy specifications of variable velocities along

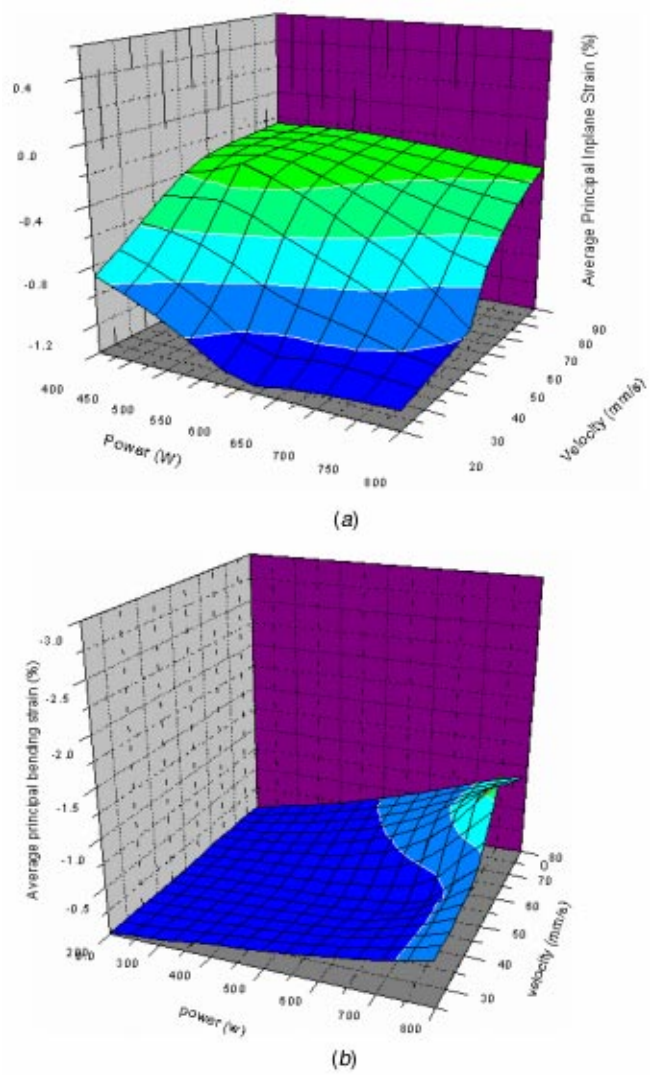


**Fig. 8 FEM-determined relationship between laser power, scanning velocity and (*a*) minimal principal in-plane strain, and (*b*) minimal principal bending strain, both averaged within the heating zone equal to the laser beam size of 4 mm (1010 mild steel sheet of 0.89 mm thick)**

a path with smooth transitions from segment to segment. Figure 10 shows the formed pillow and saddle shape under these conditions. A coordinate measuring machine (CMM) is used to measure the geometry of the formed shapes. Figure 11 compares the geometry of formed shape and desired shape. Only the geometry of top surface of the plate is measured and a general agreement is seen. However, there is about 5–10% underestimate. The discrepancy is thought due to many factors and difficult to pinpoint. Possible sources of errors include approximation of 3D strain as plain strain in laser forming, and lumped method to average the principal strains and approximate the laser power and scanning velocity.

## 6 Further Discussions

From Eq. (2), it is seen that the magnitude of bending strain increases with plate thickness. When the thickness is small, scanning paths are predominantly decided by principal in-plane strains, as the case for the two desired shapes discussed so far. When the thickness of the plate increases (but still considered as a thin plate so that this work is still applicable) and the principal bending strain becomes more dominant, it is necessary to consider

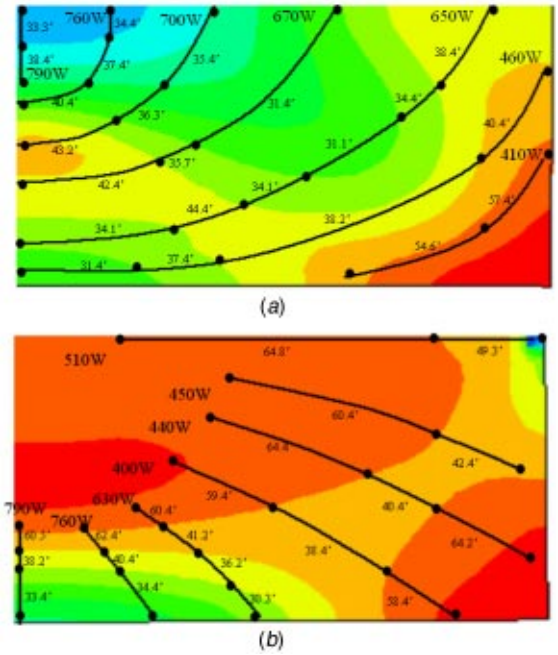


**Fig. 9 Heating condition (laser power level in W and scanning velocity in mm/s (indicated by sign ' ) indicated along scanning paths and superposed on magnitude contour plots of minimal-principal in-plane strain for (*a*) pillow shape, and (*b*) saddle shape (*a* quarter of plates shown due to symmetry and see Figs. 5.4*a* and 5.5*a* color scales)**

the effects of the bending strain. To demonstrate the point, the thickness of the pillow and saddle shapes increases from 0.89 mm to 5 mm and the minimal principal in-plane and bending strains are similarly calculated are shown in Figs. 12 and 13 for pillow and saddle shapes, respectively. It is seen that the principal bending strain is comparable to the principal in-plane strain now. The scanning paths should then be determined taking into account of the vector field of both minimal principal in-plane strain and minimal principal bending strain, perhaps the direction of bending strain needs to carry more weight because under temperature gradient mechanism bending strains produced in laser forming of relatively thicker plates is more significant. However, more work is needed.

As mentioned before, laser scanning paths for a desired shape are not unique. In this work, laser scanning paths are chosen to be perpendicular to the minimal principal in-plane strain direction. However, it is postulated that the scanning paths could also be chosen to be perpendicular to the maximum principal strain direction. This is consistent with the results from Magee et al., [15], who found that both radial and circumferential laser scanning paths could be used to form spherical dome shapes from initially flat plates of mild steel. A close look shows that, since they used a constant power and velocity level for a path, local curvatures are different whether radial or circumferential paths are used. In this work, velocities are allowed to vary along a path. This provides the capability to curve a plate not only around but also along the path. This in turn provides the capability of using different sets of scanning paths but generating similar local curvatures.

Magee et al., [15] summarized several empirical rules for sequencing laser paths for laser forming of symmetrical shapes such as spherical dome shapes, such as geometrical symmetry should be reached as soon as possible after the initial irradiation. The scanning sequence that was highly recommended is that radial paths are applied first, followed by a set of circumferential paths. Although their work is concerned with a special class of geometry, it signifies the issue of path sequencing, especially when paths crossover. In this work, the main objective is to design laser scan-

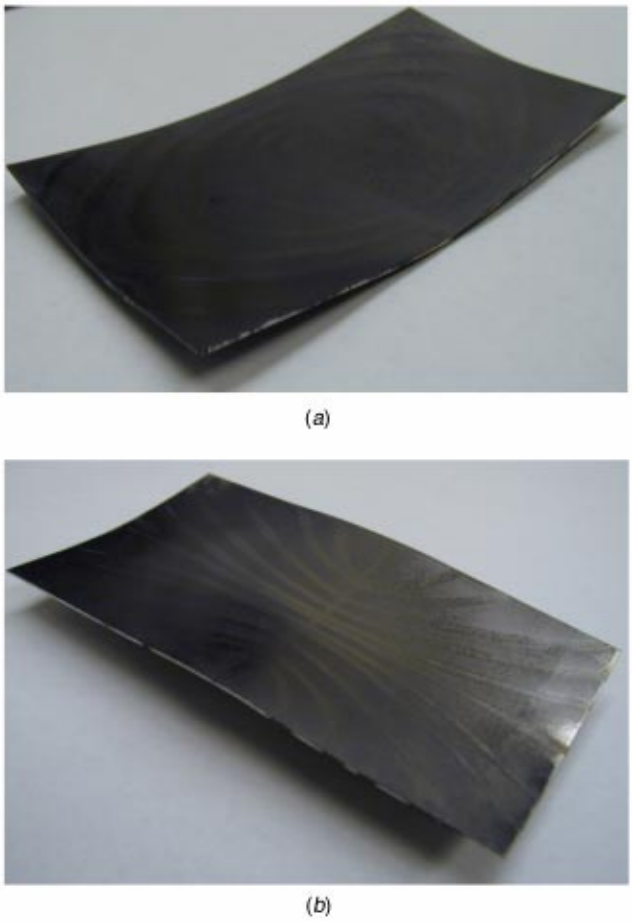


**Fig. 10 Laser formed AISI1010 steel thin plates (dimension: 140*80*0.89 mm$^3$) (*a*) pillow shape, & (*b*) saddle shape using scanning paths and heat conditions indicated in Fig. 9.**

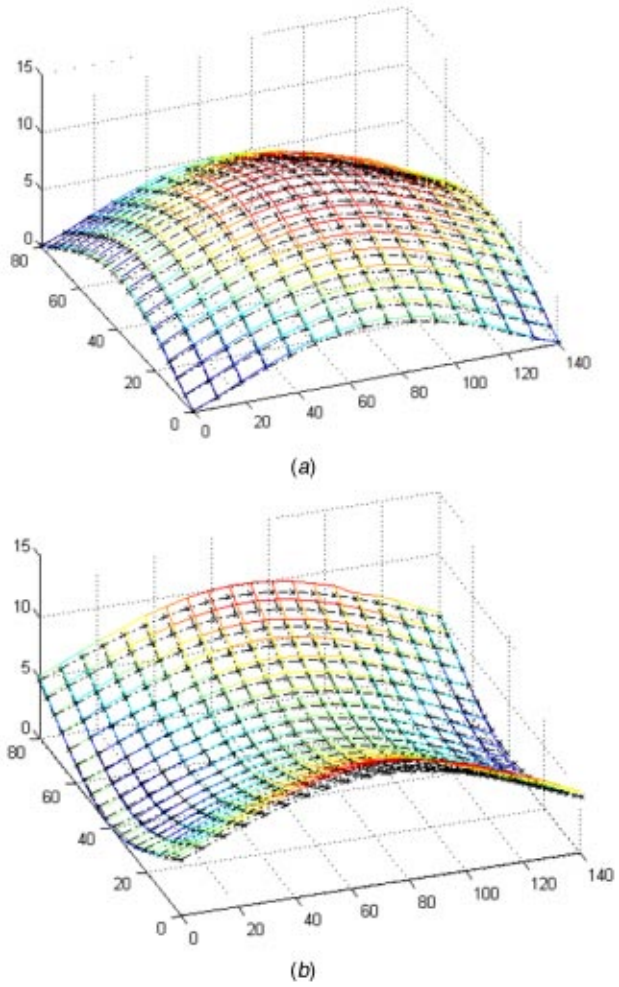


**Fig. 11 Comparison of top-surface geometry of formed plate (in dotted lines) and desired shape (in solid lines) for (*a*) pillow shape, and (*b*) saddle shape. The formed plates were measured by CMM.**

ning paths and laser heating condition. It is assumed that the geometry changes due to each scan are independent to each other when using a database based on independent scans to determine a heat condition. There is no crossover of paths in this work. In experiments, a plate is clamped at one corner and paths farthest away from the corner are scanned first and closest ones last primarily to keep the laser focus plane unchanged.

## 7 Conclusions

In this paper, a process design approach is developed for laser forming of doubly curved thin plates. Strain field determination via large-deformation elastic FEM is shown to be valid and effective. It is theoretically shown and FEM validated that the strain field determination for a desired shape can be achieved independent of any material properties including elastic properties like Young's modulus. Using minimal principal in-plane strain directions to generate scanning paths is shown to be simple. Using a database of as minimal principal in-plane strain magnitudes as function of laser power and velocity and also based on practical considerations, issues surrounding multiple solutions are resolved in determining a heating condition. It is demonstrated through two distinctively different doubly curved shapes of thin plate that the approach is effective in designing scanning paths and heating condition for laser forming process and the results agree with experimental measurements.

## Appendix

It is shown in this section that, for large-deflection of thin plates, a strain field required for planar development of a desired shape can be determined independent of material properties including Young modules $E$. The assumptions large-deflection of thin plates are (1) the material of the plate is elastic, homogenous, and isotropic; and (2) the straight lines, initially normal to the midplane before bending, remain straight and normal to the midplane during the deformation and the length of such element is not altered. This means that the vertical shear strains $\gamma_{xz}$ and $\gamma_{yz}$, are negligible and the normal strain $\varepsilon_{zz}$ is also omitted. Under these assumptions, the total strains can be expressed as a summation of the in-plane strains $\varepsilon^0_{xx}$, $\varepsilon^0_{yy}$, and $\gamma^0_{xy}$ and bending strains $\varepsilon^1_{xx}$, $\varepsilon^1_{yy}$, and $\gamma^1_{xy}$ as shown in Eq. (1).

Summing the three in-plane strains equations gives

$$\frac{\partial^2 \varepsilon^0_{xx}}{\partial y^2}+\frac{\partial^2 \varepsilon^0_{yy}}{\partial x^2}-\frac{\partial^2 \gamma^0_{xy}}{\partial x \partial y}=\left(\frac{\partial^2 w_0}{\partial x \partial y}\right)^2-\frac{\partial^2 w_0}{\partial x^2}\frac{\partial^2 w_0}{\partial y^2} \qquad (A1)$$

Substituting the relations between strains and membrane forces $N_x$, $N_y$, and $N_{xy}$, according to Hooke's law, are of the form:

$$\varepsilon^0_{xx}=\frac{1}{Eh}(N_x-\nu N_y), \quad \varepsilon^0_{yy}=\frac{1}{Eh}(N_y-\nu N_x), \quad \gamma^0_{xy}=\frac{N_{xy}}{Gh} \qquad (A2)$$

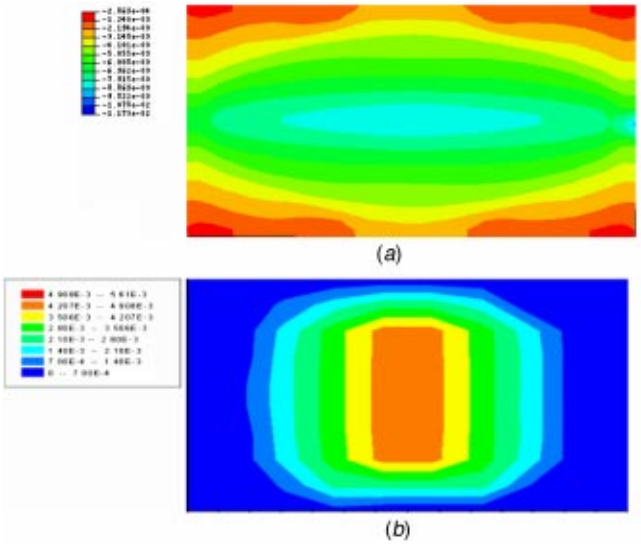

**Fig. 12 (*a*) Minimal principal in-plane strain, and (*b*) minimal principal bending strain for the pillow shape of thicker plate (dimension: 140*80*5 mm$^3$)**

where $E$ is Young's modulus, $G$ is shear modulus, and $\nu$ is Poisson ratio, and stress function $\phi$ for the membrane forces

$$N_x=\frac{\partial^2\phi}{\partial y^2},\quad N_y=\frac{\partial^2\phi}{\partial x^2},\quad N_{xy}=-\frac{\partial^2\phi}{\partial x\partial y} \tag{A3}$$

into Eqs. (*A*1), one obtains the equation of compatibility of deformation, which allows expressing $u_0$ and $v_0$ in terms of $w_0$.

$$\frac{\partial^4\phi}{\partial x^4}+2\frac{\partial^4\phi}{\partial x^2\partial y^2}+\frac{\partial^4\phi}{\partial y^4}=Eh\left[\left(\frac{\partial^2 w_0}{\partial x\partial y}\right)^2-\frac{\partial^2 w_0}{\partial x^2}\frac{\partial^2 w_0}{\partial y^2}\right] \tag{A4}$$

Considering the equilibrium of an thin plate element, which experiences the membrane forces $N_x$, $N_y$, and $N_{xy}$, and is also subjected to a lateral load $P(x,y)$ in the $z$ direction. Taking into account Eq. (*A*3), the force equilibrium in the $z$ directions leads to:

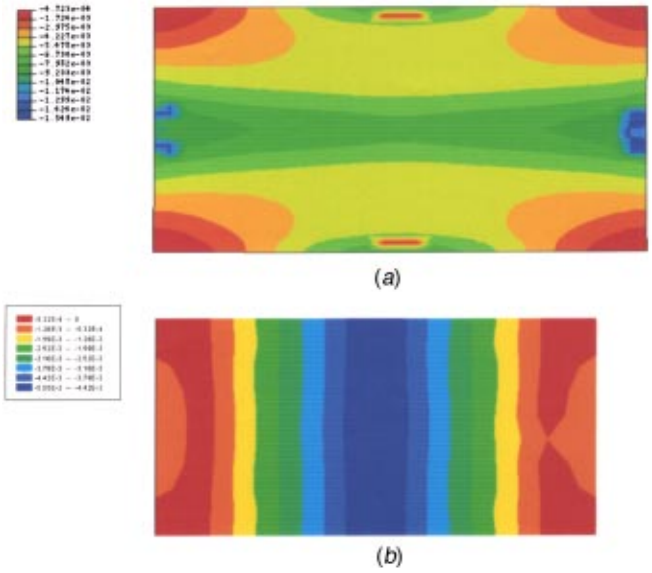

**Fig. 13 (*a*) Minimal principal in-plane strain, and (*b*) minimal principal bending strain for the saddle shape of thicker plate (dimension: 140*80*5 mm$^3$)**

$$\frac{\partial^4 w_0}{\partial x^4}+2\frac{\partial^4 w_0}{\partial x^2\partial y^2}+\frac{\partial^4 w_0}{\partial y^4}=\frac{1}{D}\left[P+\frac{\partial^2\phi}{\partial y^2}\frac{\partial^2 w_0}{\partial x^2}+\frac{\partial^2\phi}{\partial x^2}\frac{\partial^2 w_0}{\partial y^2}-2\frac{\partial^2\phi}{\partial x\partial y}\frac{\partial^2 w_0}{\partial x\partial y}\right] \tag{A5}$$

where $D=Eh^3/12(1-\nu^2)$, is the flexural rigidity of the plate. Let $\varphi=\phi/E$, Eqs. (*A*4) and (*A*5) take the form

$$\frac{\partial^4\varphi}{\partial x^4}+2\frac{\partial^4\varphi}{\partial x^2\partial y^2}+\frac{\partial^4\varphi}{\partial y^4}=h\left[\left(\frac{\partial^2 w_0}{\partial x\partial y}\right)^2-\frac{\partial^2 w_0}{\partial x^2}\frac{\partial^2 w_0}{\partial y^2}\right] \tag{A6a}$$

$$\frac{\partial^4 w_0}{\partial x^4}+2\frac{\partial^4 w_0}{\partial x^2\partial y^2}+\frac{\partial^4 w_0}{\partial y^4}=\frac{1}{D'}\left[P'+\frac{\partial^2\varphi}{\partial y^2}\frac{\partial^2 w_0}{\partial x^2}+\frac{\partial^2\varphi}{\partial x^2}\frac{\partial^2 w_0}{\partial y^2}-2\frac{\partial^2\varphi}{\partial x\partial y}\frac{\partial^2 w_0}{\partial x\partial y}\right] \tag{A6b}$$

where $D'=D/E=h^3/12(1-\nu^2)$, and $P'=P/E$. Equations (*A*6) are the governing differential equations for thin plate deflection. As seen from Eq. (*A*6), once a desired shape is given, deflection $w_0$, and curvatures $\partial^2 w_0/\partial x^2$, $\partial^2 w_0/\partial y^2$, and $\partial^2 w_0/\partial x\partial y$ are known, and therefore $\varphi$ and $P'$ can be calculated under appropriate boundary conditions independent of material properties including Young's modulus $E$. Once $\varphi$ is solved, the in-plane strains $\varepsilon^0_{xx}$, $\varepsilon^0_{yy}$, and $\gamma^0_{xy}$ can be determined again independent of material properties including Young's modulus $E$, taking into account of Eqs. (*A*2), (*A*3) and $\varphi=\phi/E$ as follows

$$\varepsilon^0_{xx}=\frac{1}{h}\left(\frac{\partial^2\varphi}{\partial y^2}-\nu\frac{\partial^2\varphi}{\partial x^2}\right),\quad \varepsilon^0_{yy}=\frac{1}{h}\left(\frac{\partial^2\varphi}{\partial x^2}-\nu\frac{\partial^2\varphi}{\partial y^2}\right),$$

$$\gamma^0_{xy}=-\frac{2(1+\nu)}{h}\frac{\partial^2\varphi}{\partial x\partial y} \tag{A7}$$

Their determination does depend on Poisson ratio$\nu$, but $\nu$ is a geometric quantity relating strains. Bending strains ($\varepsilon^1_{xx}$, $\varepsilon^1_{yy}$, $\gamma^1_{xy}$) can be determined in the same form as Eq. (2), and are independent of both Young's modulus and Poisson ratio.

## References


[1] Hsiao, Y.-C., Shimizu, H., Firth, L., Maher, W., and Masubuchi, K., 1997, "Finite Element Modeling of Laser Forming," Section A-ICALEO 1997, pp. 31–40.

[2] Magee, J., Watkins, K. G., and Steen, W. M., 1998, "Advances in laser Forming," J. Laser Appl., **10**, pp. 235–246.

[3] Bao, J., and Yao, Y. L., 1999, "Analysis and Predication of Edge Effects in Laser Bending," *Proceedings of ICALEO 1999*, Section C, pp. 186–195.

[4] Li, W., and Yao, Y. L., 2000, "Numerical and Experimental Study of Strain Rate Effects in Laser Forming," ASME J. Manuf. Sci. Eng., **122**, August, pp. 445–451.

[5] Li, W., and Yao, Y. L., 2000, "Convex Laser Forming With High Certainty," *Trans. of the North American Manufacturing Research Conference of SME XXVIII*, pp. 33–38.

[6] Li, W., and Yao, Y. L., 2001, "Laser Bending of Tubes: Mechanism, Analysis and Prediction," ASME J. Manuf. Sci. Eng., **123**(4), pp. 674–681.

[7] Ueda, K., Murakawa, H., Rashwan, A. M., Okumoto, Y., and Kamichika, R., 1994, "Development of Computer-Aided Process Planning System for Plate Bending by Line Heating (Report 1)—Relation Between Final Form of Plate and Inherent Strain," Journal of Ship Production, **10**(1), pp. 59–67.

[8] Ueda, K., Murakawa, H., Rashwan, A. M., Okumoto, Y., and Kamichika, R., 1994, "Development of Computer-aided Process Planning System for Plate Bending by Line Heating (Report 2)—Practice for Plate Bending in Shipyard Viewed from Aspect of Inherent Strain," Journal of Ship Production, **10**(4), pp. 239–247.

[9] Ueda, K., Murakawa, H., Rashwan, A. M., Okumoto, Y., and Kamichika, R., 1994, "Development of Computer-aided Process Planning System for Plate Bending by Line Heating (Report 3)—Relation Between Heating Condition and Deformation," Journal of Ship Production, **10**(4), pp. 248–257.

[10] Jang, C. D., and Moon, S. C., 1998, "An Algorithm to Determine Heating Lines for Plate Forming by Line Heating Method," Journal of Ship Production, **14**(4), pp. 238–245.

[11] Shimizu, H., 1997, "A Heating Process Algorithm for Metal Forming by a Moving Heat Source," M.S. Thesis, MIT.

[12] Yu, G., Patrikalakis, N. M., and Maekawa, T., 2000, ''Optimal Development of Doubly Curved Surfaces,'' Computer Aided Geometric Design, **17**, pp. 545–577.
[13] Cheng, J., and Yao, Y. L., 2001, ''Process Synthesis of Laser Forming by Genetic Algorithms,'' *Proceedings of ICALEO 2001*, Section D 604.
[14] Liu, C., and Yao, Y. L., 2002, ''Optimal and Robust Design of Laser Forming Process,'' *North American Manufacturing Research Institute of SME*, May, in press.
[15] Magee, J., Watkins, K. G., and Hennige, T., 1999, ''Symmetrical Laser forming,'' *Proceedings of ICALEO 1999*, pp. 77–86.